BULLETIN OF THE POLISH ACADEMY OF SCIENCES
TECHNICAL SCIENCES, Vol. 69(5), 2021, Article number: e137507
DOI: 10.24425/bpasts.2021.137507

Characterization of morphology and optical properties of SnO_2 nanowires prepared by electrospinning

Tomasz TAŃSKI, Weronika SMOK*, and Wiktor MATYSIAK

Department of Engineering Material and Biomaterials, Silesian University of Technology, ul. Konarskiego 18A, 44-100 Gliwice, Poland

Abstract. The growing interest in one-dimensional tin oxide-based nanomaterials boosts research on both high-quality nanomaterials as well as production methods. This is due to the fact that they present unique electrical and optical properties that enable their application in various (opto) electronic devices. Thus, the aim of the paper was to produce ceramic SnO_2 nanowires using electrospinning with the calcination method, and to investigate the influence of the calcination temperature on the morphology, structure and optical properties of the obtained material. A scanning electron microscope (SEM) and Fourier-transform infrared spectroscopy (FTIR) were used to examine the morphology and chemical structure of obtained nanomaterials. The optical properties of manufactured one-dimensional nanostructures were investigated using UV-Vis spectroscopy. Moreover, based on the UV-Vis spectra, the energy band gap of the prepared nanowires was determined. The analysis of the morphology of the obtained nanowires showed that both the concentration of the precursor in the spinning solution and the calcination temperature have a significant impact on the diameter of the nanowires and, consequently, on their optical properties.

Key words: nanowires; nanofibers; electrospinning; tin oxide; optical properties.

1. INTRODUCTION

Among the most intensively investigated metal oxide semiconductors (MOS) such as TiO_2, ZnO, Fe_2O_3, WO_3, and In_2O_3, SnO_2 is the most important because of its wide application potential, confirmed by numerous research studies over the last decade [1–6].

SnO_2 is an n-type semiconductor with a wide energy band gap in the range of 3.5–4.75 eV and high exciton binding energy (130 meV), typically optically transparent with high electron mobility $\left(240\ \mathrm{cm^2\ V^{-1}\ s^{-1}}\right)$ and refractive index of 2.0. Additionally, SnO_2 exhibits high mechanical, thermal and chemical stability [7–9]. Tin oxide is an important oxide in (opto)electronic technologies involving efficient photocatalysis, gas sensors, thin-film transistors and other transparent electronic devices [10, 11].

Currently, scientists are focused on the study of one-dimensional (1D) MOS due to their better optical and electrical properties than those of bulk materials. Nanostructured 1D tin oxide semiconductors have been well studied with regard to their synthesis methods. There are many varieties of 1D SnO_2 fabrication techniques such as the solvo- and hydrothermal one, microwave technique, chemical vapor deposition, template synthesis, electrospinning with calcination and numerous others [12–16]. Electrospinning is one of the best-studied methods for the synthesis of MOS 1D nanostructures and the development of semiconductor devices because of its simplicity and low cost [17, 18]. Moreover, electrospinning provides a large specific surface area, high porosity and tunable structure of the produced materials [19]. In the first step of this method, nanofibrous mats are prepared by electrospinning from the solution of a tin oxide precursor and the selected polymer. Next step involves calcination at a temperature in the range of 400–700°C to remove the polymer matrix and obtain pristine, polycrystalline SnO_2 nanowires [20, 21].

Previous research indicates the wide application potential of electrospun SnO_2 nanowires and the ease of modifying their properties by doping with ions, other MOS or carbon materials [22–30]. In their work, Zhang *et al*. [31] described the method of producing SnO_2 nanofibers using electrospinning and applying them in the construction of gas sensors. The sensor fabricated from these fibers exhibits excellent toluene sensing properties combined with fast response and recovery time. Li *et al*. [32] indicated that porous SnO_2 nanobelts are extremely effective in detecting acetone, while Cheng *et al*. [33] showed that core-shell SnO_2 nanofibers-based sensors can be used to detect ethanol. Multiple studies confirmed that doping with NiO, ZnO, TiO_2, Al_2O_3 and CuO improves sensing properties of the sensors based on SnO_2 [34–38]. The application of SnO_2 nanofibers to the anodes of lithium-ion batteries (LIB) was presented by Hwang *et al*. [39], who showed that LIB based on nanofibers are characterized by higher efficiency than SnO_2 nanoparticles-based LIB. The efficiency of LIB with a SnO_2 anode can be significantly increased by modifying it with carbon materials, e.g. in the form of carbon coating, or by doping the spinning solution with graphene [40, 41]. Due

*e-mail: weronika.smok@polsl.pl

Manuscript submitted 2021-02-26, revised 2021-03-31, initially accepted for publication 2021-04-08, published in October 2021

to its large specific surface area and superior charge transport characteristics, 1D SnO_2 can also be used as a photoanode in dye-sensitized solar cells, as proved by Wali *et al*. [42].

Herein, the authors present a simple, low-cost method for the synthesis of 1D SnO_2 nanostructures. For the first time, in this work, the authors focused on the investigation of the effect of precursor concentration and calcination temperature on the morphology and optical properties of the manufactured SnO_2 nanomaterials. The prepared nanostructures exhibited nanograined wire-like morphologies. The morphology and energy bandgap of the prepared nanomaterials were found to be controllable with temperature of the thermal treatment.

2. MATERIALS AND METHODS

In order to prepare the spinning solutions for 1D tin oxide nanostructures, the following were used: poly(vinylpyrrolidone) (PVP, purity of 99%), *N*, *N*-dimethylformamide (DMF, purity of 99.8%), ethanol (EtOH, purity of 99.8%) and tin chloride pentahydrate ($SnCl_4 \cdot 5H_2O$, purity of 98%) – all provided by Sigma-Aldrich.

Four identical solutions of 8 wt.% PVP in ethanol were prepared, at the same time, four solutions of $SnCl_4 \cdot 5H_2O$ in DMF differing in the concentration of the precursor were prepared in such a way that after mixing the polymer and precursor solutions, PVP/$SnCl_4 \cdot 5H_2O$ solutions with the following polymer/precursor weight ratios: 2:1, 1:1, 1:2 and 1:3 were obtained. Then, they were mixed for 72 h using a magnetic stirrer until homogeneous solutions were prepared. The solutions were placed successively in the pump of the FLOW – Nanotechnology Solutions Electrospinner 2.2.0–500 device, which was used to prepare four PVP/$SnCl_4$ nanofibrous composite mats (Table 1).

Table 1
Samples naming depending on the polymer: precursor ratio and calcination temperature

PVP:$SnCl_4$ wt. ratio	Sample name before calcination	Sample name after calcination in 500°C	Sample name after calcination in 600°C
2:1	PVPA	500A	600A
1:1	PVPB	500B	600B
1:2	PVPC	500C	600C
1:3	PVPD	500D	600D

As-spun PVP/$SnCl_4$ samples were left in room conditions to dry. In the second step, calcination in an FCF 7 SHM CZYLOK muffle furnace at temperatures of 500 and 600°C with a heating rate of 2°C/min for 5 h was performed. Then, the samples produced were left in a furnace to cool down completely. Thus, eight samples of SnO_2 one-dimensional nanostructures were manufactured (Table 1). In order to determine the morphology of the prepared composite nanofibers and ceramic nanowires, a Zeiss Supra 35 scanning electron microscope (SEM) was used. Hundredfold diameter measurement was carried on randomly selected PVP/$SnCl_4$ nanofibers and SnO_2 nanowires, based on the SEM images, and the results were presented in the form of a histogram. To analyze the oscillatory transitions of atoms vibrating between the oscillatory levels in the molecules of the fabricated nanomaterials, and to determine the functional groups, Fourier-transform infrared spectroscopy (FTIR) (Nicolet™ iS™ 50 FTIR Spectrometer, Thermo Fisher Scientific) was used. Analysis of the optical properties of SnO_2 nanowires was conducted on the basis of absorbance measurements obtained using the UV-Vis Evolution 220 spectrophotometer from Thermo-Scientific Company. Moreover, the energy band gap (E_g) of the prepared one-dimensional nanostructures was evaluated using the methods presented in works [43–46].

3. MRESULTS AND DISCUSSION

3.1. Morphology analysis

Using a scanning electron microscope, the topography of the surface of electrospun nanofibrous composite PVP/$SnCl_4$ mats was imaged (Fig. 1). The analysis of the morphology and structure of the materials showed that regardless of the polymer to precursor weight ratio, the nanofibers were smooth, homogeneous, free from beads and pores, and showed a constant diameter along the entire length of the nanofiber. However, based on hundredfold measurements of the diameters of randomly selected fibers, a significant effect of the concentration of the precursor on the average diameter of the fiber was observed. PVPA nanofibers obtained from the solution with the smallest amount of the precursor had diameters ranging from 20 to 120 nm, with an average diameter of 59 nm, which is the smallest diameter observed among all composite nanofiber samples (Fig. 1).

As the precursor concentration increases, the average diameter of nanofibers increases from 134 nm through 180 nm up to 251 nm for samples with a polymer to precursor ratio of 1:1, 1:2 and 1:3, respectively (Fig. 1). This phenomenon was also observed in the process of electrospinning of other metal oxides, including ZnO, WO_3, SiO_2 and TiO_2 nanowires, and SnO_2 hybrid nanowires [20, 47–50].

The analysis of the morphology of the nanomaterials after calcination at 500°C showed that nano-grained 1D structures in the form of nanowires of the constant diameter along the entire length were produced, and no defects or sintered wires were observed, which proves that the calcination temperature was selected properly (Fig. 1). Thermal treatment of the spun PVP/$SnCl_4$ composite nanofibers at 500°C for 5 h allowed to obtain SnO_2 nanowires with a diameter distinctly smaller than in the case of nanostructures before calcination, which is the result of PVP degradation (Fig. 1). Depending on the polymer to precursor ratio in the solution used to obtain SnO_2 nanowires, the average diameter of the nanowires ranged from 61 to 143 nm. As in the case of nanofibers before calcination, an increase in the diameter of nanowires was observed with an increase in the concentration of $SnCl_4$. This results from a greater amount of starting material available to form the final 1D SnO_2 product [48].

One-dimensional SnO_2 nanostructures without defects were also obtained using a higher calcination temperature of 600°C, which confirmed that the formation of SnO_2 nanowires is also possible at this temperature [51]. A hundredfold measurement of the diameters of randomly selected nanowires confirmed that the use of higher temperature also allowed for complete degradation of the organic phase and, as a result, for the fabrication of wires with an average diameter not exceeding 57 nm, regardless of the polymer to precursor ratio in the spinning solution used to produce nanowires. In addition, it can be observed that the con-

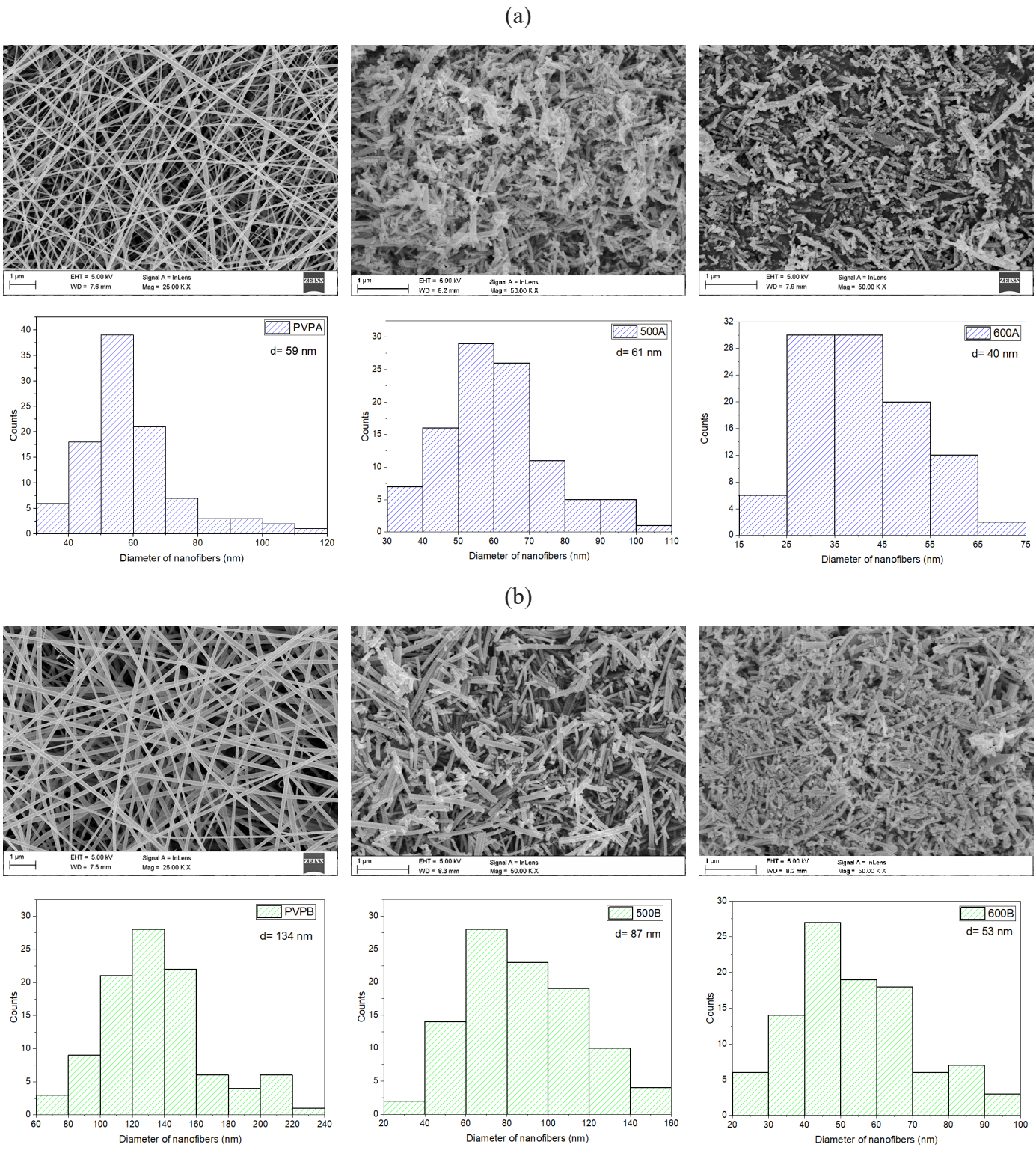

Fig. 1. SEM images of the fabricated (from left) PVP/$SnCl_4$ nanofibers and nanowires calcined at 500 and 600°C with corresponding histograms showing the distribution of diameter values below, obtained from spinning solutions with polymer to precursor ratio of: a) 2:1, b) 1:1, c) 1:2, d) 1:3

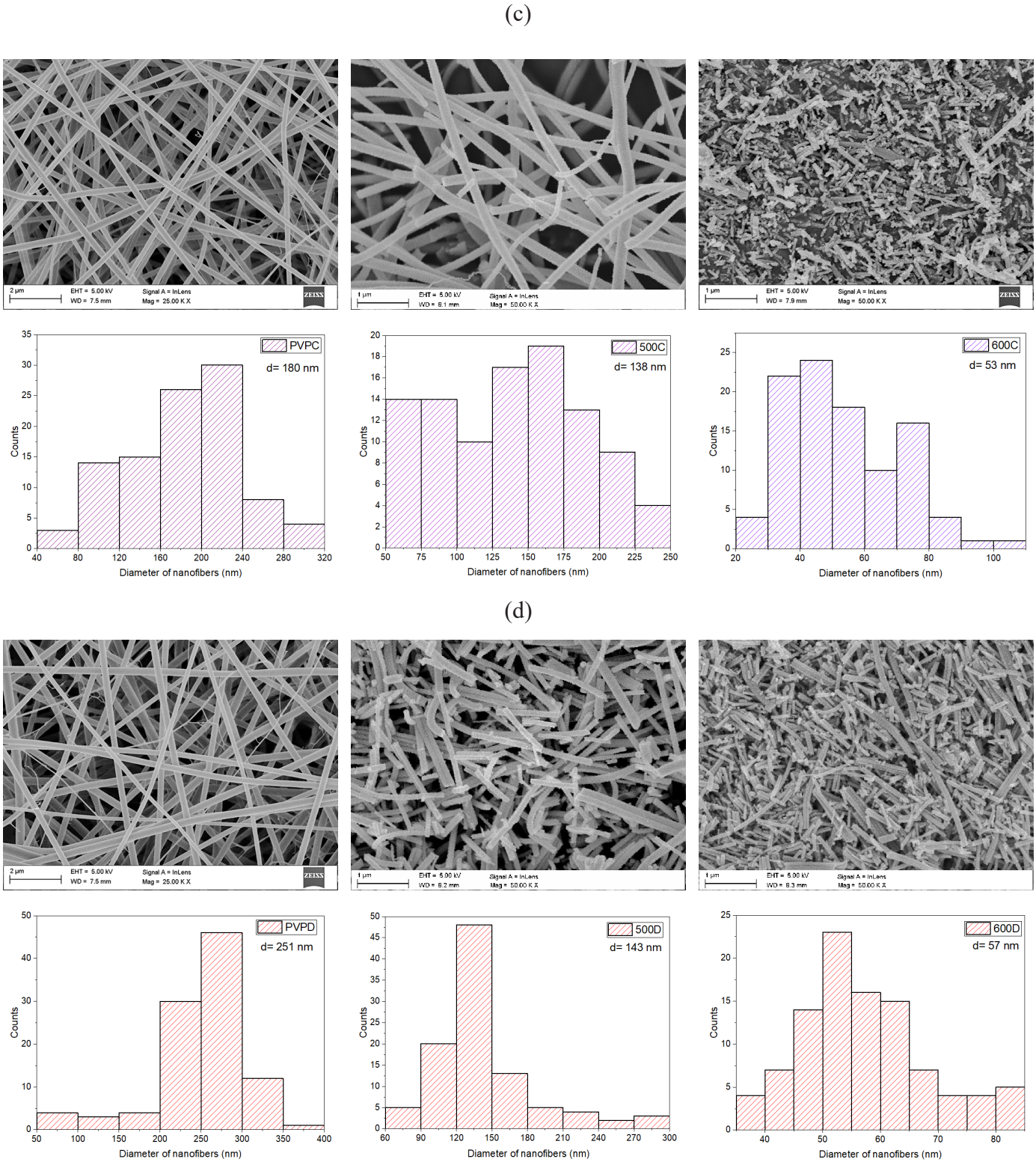

Fig. 1. SEM images of the fabricated (from left) PVP/$SnCl_4$ nanofibers and nanowires calcined at 500 and 600°C with corresponding histograms showing the distribution of diameter values below, obtained from spinning solutions with polymer to precursor ratio of: a) 2:1, b) 1:1, c) 1:2, d) 1:3

centration of the precursor in the solution does not significantly affect the diameter of the nanowires after calcination at 600°C as in the case of nanowires calcined at 500°C, the calculated average diameters for samples 600A, 600B, 600C and 600D were 40, 53, 53, 57 nm, respectively. These values were similar, while in the case of two samples obtained from the solution with the highest concentrations of the precursor, nanostructures with a diameter exceeding 100 nm were observed.

3.2. FTIR analysis

In order to obtain information about the transitions in the molecule between the oscillatory levels and to identify the functional groups present in the chemical structure of the electrospun composite PVP/$SnCl_4$ nanofibers and the SnO_2 ceramic nanowires, an analysis of FTIR spectra of transmittance as a function of the wavenumber in the range from 3,500 to 500 cm^{-1} (Fig. 2) was performed. The spectrum recorded for each of the PVPA-D samples shows the peaks characteristic for PVP from C-N stretching vibrations $(1{,}301–1{,}288\ cm^{-1})$, CH_2 scissor vibrations $(1{,}454–1{,}439\ cm^{-1})$, C = O stretching vibrations $(1{,}646–1{,}621\ cm^{-1})$ and asymmetric CH_2 stretching vibrations in the positions of 2,962–2,942 cm^{-1} (Fig. 2a–d). According to the literature, the spectra obtained for nanowires calcined at both 500 and 600°C do not show the peaks characteristic of the PVP polymer, which clearly confirms the complete removal of the polymer. In addition, broad peaks at the 560–620 cm^{-1} position can be observed in the spectra recorded for samples 500A–D and 600A–D, corresponding to the Sn-O bond which is characteristic of SnO_2 and indicates the formation of SnO_2 nanowires for each sample (Fig. 2 a–d).

3.3. Optical properties analysis

Analysis of optical properties of the obtained 1D SnO_2 nanostructures was performed on the basis of recorded absorbance spectra in the function of electromagnetic radiation of a wavelength range of 290–700 nm (Fig. 3).

The spectral characteristics recorded for one-dimensional SnO_2 500A-D nanostructures were characterized, irrespective of the polymer to precursor ratio, by the presence of an absorption edge in the near-ultraviolet region (Fig. 3a). The absorption maximum of obtained nanowires was found for waves of the wavelength of 306–323 nm. It can be observed that the absorbance level increased with the increasing concentration of the precursor in the spinning solution used for nanowires preparation. The presented spectral lines and the corresponding absorption maxima within UV radiation are characteristic for the UV-Vis spectra of tin oxide [51].

A significant increase in absorption of electromagnetic radiation in the UV region was observed for SnO_2 nanowires calcined at 600°C (Fig. 3b), which can be explained by the greater thickness of this sample. Despite the smaller diameter of nanofibers 600A–D than the diameter of 500A–D, the prepa-

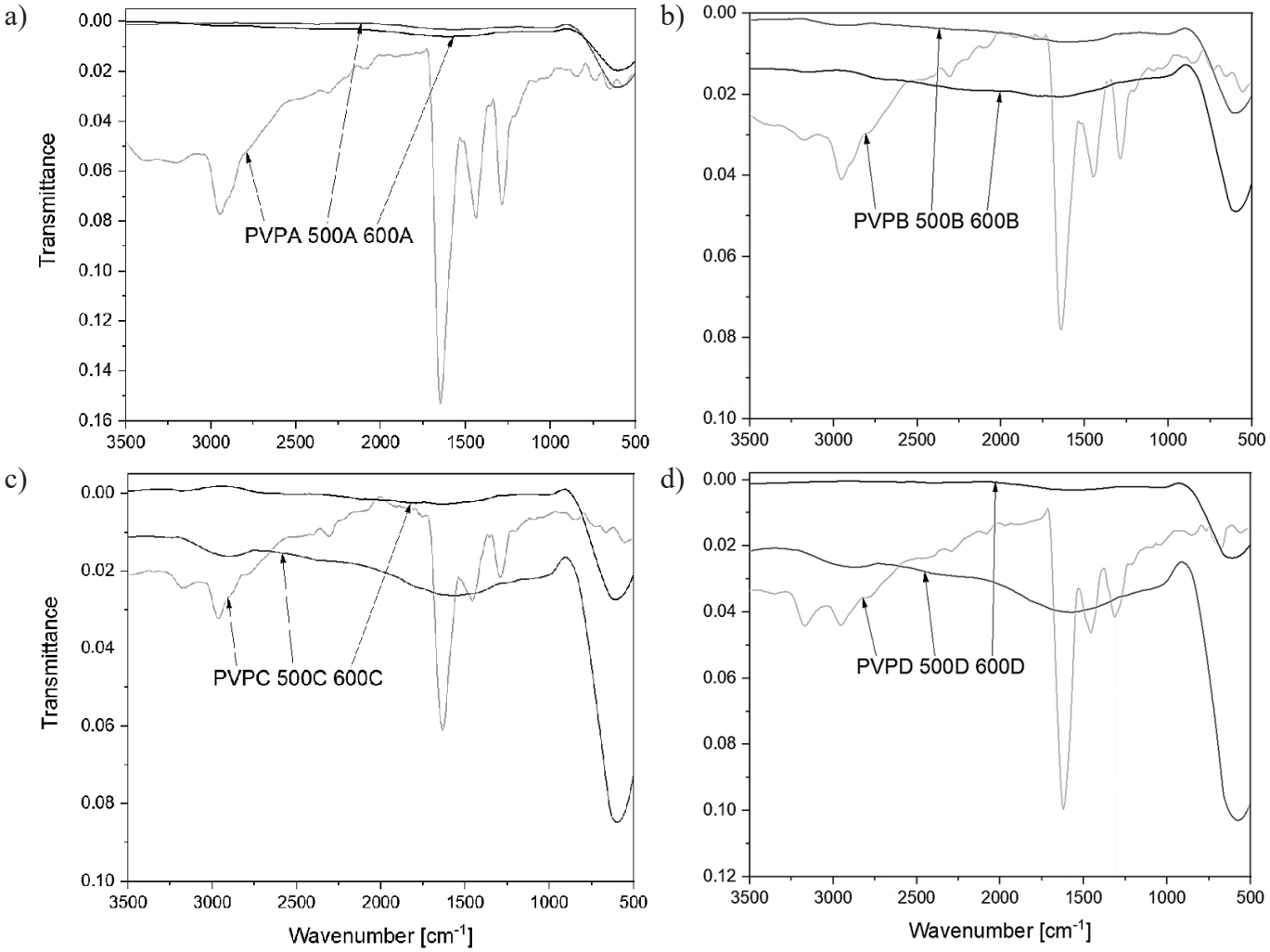

Fig. 2. FTIR spectra recorded for composite PVP/$SnCl_4$ nanofibers and nanowires calcined at 500 and 600°C, values obtained from spinning solutions with polymer to precursor ratio of: a) 2:1, b) 1:1, c) 1:2, d) 1:3

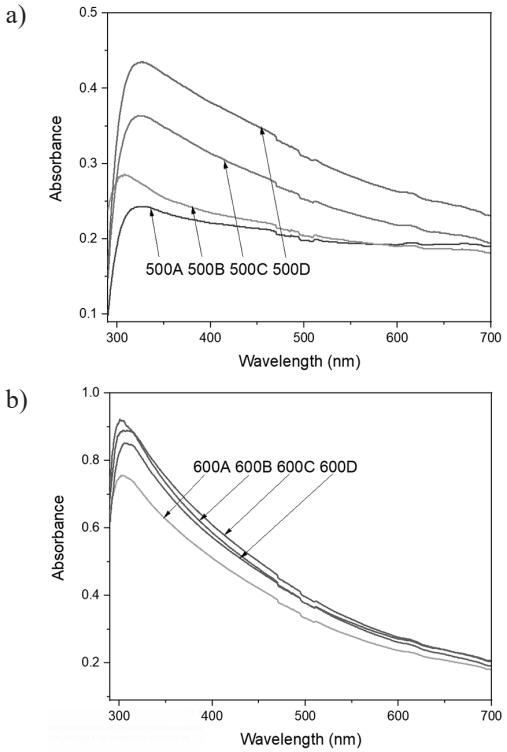

Fig. 3. UV-Vis spectra for SnO_2 nanowires obtained after calcination at: a) 500°C, b) 600°C

ration of samples for optical studies caused that the thickness of the analyzed samples was greater. Moreover, the spectra recorded for 600A–D show a sharper absorption edge, and the absorption maximum was shifted towards electromagnetic radiation with greater energy and corresponded to a wavelength of 300–305 nm [52].

The optical band gaps were evaluated based on the absorbance spectra in the function of wavelength recorded for the SnO_2 nanostructures calcined at 500 and 600°C using the following equation (1):

$$\alpha h\upsilon = A\left(h\upsilon - E_g\right)^{\rho}, \tag{1}$$

where, α – absorption coefficient, h – Planck constant, υ – frequency of the radiation, A – constant, hν – photon energy, E_g – energy band gap of the material, ρ – coefficient depending on the type of electron transitions (the taken value was 2, which corresponds to direct transition). The band gaps were calculated using Tauc plots [2, 43]. Formulas $(\alpha h\upsilon)^2$ as a function of the quantum radiation energy obtained for SnO_2 nanowires are presented in Fig. 4. Nanowires manufactured after calcination at a lower temperature were characterized by a band gap in the range of 2.44–2.76 eV (Fig. 4a), which corresponds to the values presented in the literature [51]. Calcination at a higher temperature (600°C) allowed to obtain nanowires with a larger energy gap, ranging from 3.06 to 3.12 eV (Fig. 4b) [52].

Analysis of band structure of the manufactured SnO_2 nanowires has shown a significant influence of the calcination temperature and concentration of the precursor in the spinning solution used to produce nanostructures on the energy band gap for the analyzed nanomaterials. This is related to the morphology of nanowires – higher temperature and lower concentration provide a smaller diameter of nanowires, thus a higher energy band gap. This phenomenon is common because in one-dimensional nanostructured semiconductors the movement of the electrons is free in only one direction, but in other directions

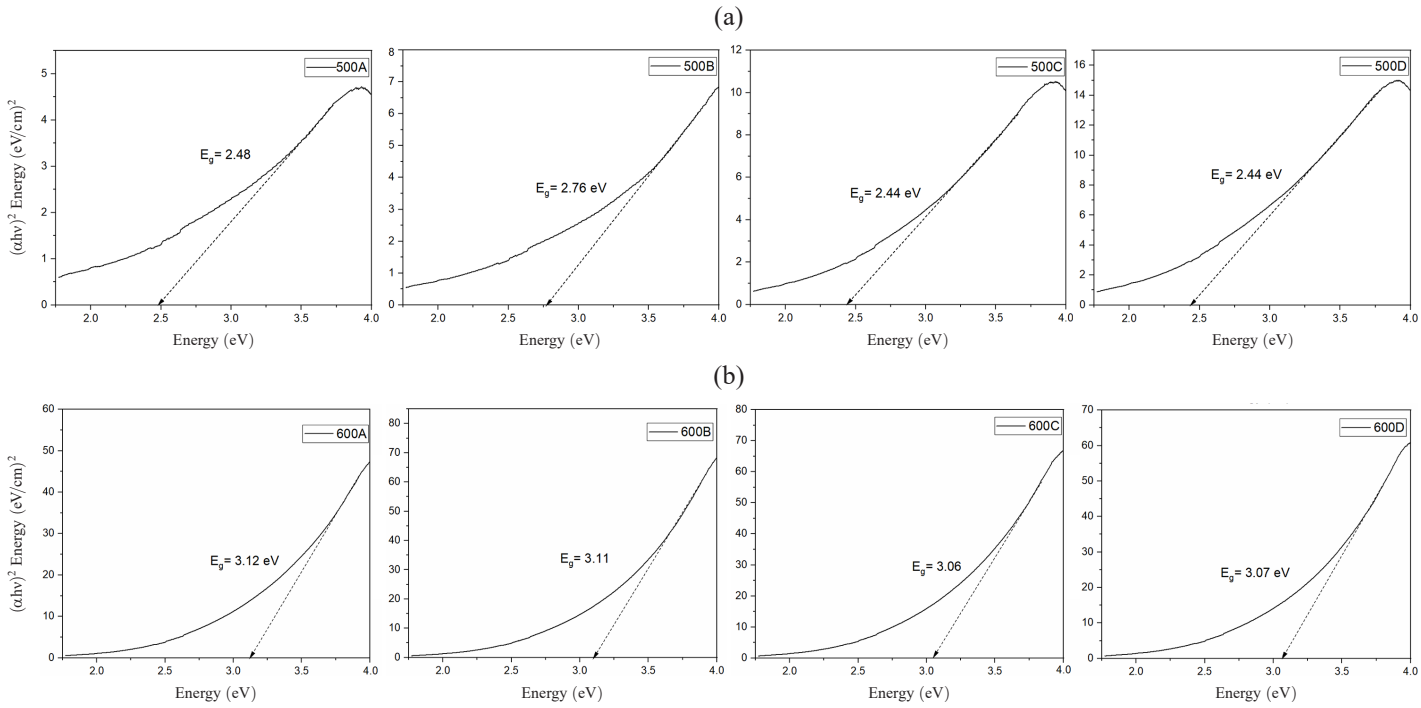

Fig. 4. Tauc plots showing the optical band gap of SnO_2 nanowires obtained after calcination at: a) 500°C, b) 600°C

quantization occurs. It is related to the change in the electronic state of the semiconductor and leads to the increase of the forbidden band, which helps the electron to transfer between the states through the shift of the position of the conduction band to lower values [53, 54].

The above investigation of the interaction of SnO_2 nanowires with electromagnetic radiation in the range of 290–700 nm clearly indicates a very effective absorption of ultraviolet radiation. Moreover, the energy band gap in the range of 2.44–3.12 rendered the fabricated nanostructures possible to be applied in advanced optoelectronic devices.

4. CONCLUSIONS

SnO_2 nanowires were successfully prepared by means of a facile electrospinning technique in combination with calcination treatment. Nanofibers with different polymer to precursor ratio in a spinning solution of 2:1, 1:1, 1:2, 1:3 were prepared and then calcined at two temperatures of 500 and 600°C. It was revealed that the variation of spinning solution parameters and calcination temperature can control the morphology and optical properties of SnO_2 nanowires. It was also observed that an increase in the precursor concentration in the spinning solution causes an increase in the diameter of the finally obtained SnO_2 nanowires from 60 to even 140 nm. In addition, the higher calcination temperature of 600°C allowed to obtain nanowires with a smaller diameter (40–57 nm) as compared to the diameter (61–143 nm) of the nanowires manufactured after treatment at 500°C. Furthermore, an increase of the absorption level and energy band gap of nanowires was observed after calcination at higher temperatures. This phenomenon was the result of the change in the absorption edge and the increase in carrier concentration.

The above considerations indicate that the fabrication parameters have a significant impact on the morphology and, consequently, on the properties of SnO_2 nanowires, which in the future may be used to construct innovative solar cells and other devices requiring good optoelectronic properties.

ACKNOWLEDGEMENTS

The publication was supported as a part of the Rector's grant in the area of scientific research and development works of the Silesian University of Technology, grant No. 10/010/RGJ19/0264.

REFERENCES

[1] W. Matysiak and T. Tański, "Novel bimodal ZnO (amorphous)/ZnO NPs (crystalline) electrospun 1D nanostructure and their optical characteristic," *Appl. Surf. Sci.*, vol. 474, pp. 232–242, Apr. 2019.

[2] P. Jarka, T. Tański, W. Matysiak, Ł. Krzemiński, B. Hajduk, and M. Bilewicz, "Manufacturing and investigation of surface morphology and optical properties of composite thin films reinforced by TiO_2, Bi_2O_3 and SiO_2 nanoparticles," *Appl. Surf. Sci.*, vol. 424, pp. 206–212, Dec. 2017.

[3] V.R. Bandi *et al.*, "Synthesis, structural and optical properties of pure and rare-earth ion doped TiO_2 nanowire arrays by a facile hydrothermal technique," *Thin Solid Films*, vol. 547, pp. 207–211, 2013.

[4] V.M.D.S. Rocha, M.D.G. Pereira, L.R. Teles, and M.O.D.G. Souza, "Effect of copper on the photocatalytic activity of semiconductor-based titanium dioxide (anatase) and hematite (α-Fe_2O_3)," *Mater. Sci. Eng. B-Solid State Mater. Adv. Technol.*, vol. 185, no. 1, pp. 13–20, Jul. 2014.

[5] Z. Tao, Y. Li, B. Zhang, G. Sun, J. Cao, and Y. Wang, "Bi-doped urchin-like In_2O_3 hollow spheres: Synthesis and improved gas sensing and visible-light photocatalytic properties," *Sensors Actuators B Chem.*, vol. 321, p. 128623, Oct. 2020.

[6] M. Parthibavarman, M. Karthik, and S. Prabhakaran, "Facile and one step synthesis of WO_3 nanorods and nanosheets as an efficient photocatalyst and humidity sensing material," *Vacuum*, vol. 155, pp. 224–232, Sep. 2018.

[7] Y. Chen *et al.*, "SnO_2-based electron transporting layer materials for perovskite solar cells: A review of recent progress," *J. Energy Chem.*, vol. 35, pp. 144–167, Aug. 2019.

[8] M. Dou and C. Persson, "Comparative study of rutile and anatase SnO_2 and TiO_2: Band-edge structures, dielectric functions, and polaron effects," *J. Appl. Phys.*, vol. 113, no. 8, p. 083703, Feb. 2013.

[9] X. Zhang *et al.*, "SnO_2 nanorod arrays with tailored area density as efficient electron transport layers for perovskite solar cells," *J. Power Sources*, vol. 402, pp. 460–467, Oct. 2018.

[10] V.S. Jahnavi, S.K. Tripathy, and A.V.N. Ramalingeswara Rao, "Structural, optical, magnetic and dielectric studies of SnO_2 nano particles in real time applications," *Phys. B Condens. Matter*, vol. 565, pp. 61–72, Jul. 2019.

[11] M.A. Yildirim, S.T. Yildirim, E.F. Sakar, and A. Ateş, "Synthesis, characterization and dielectric properties of SnO_2 thin films," *Spectrochim. Acta – Part A Mol. Biomol. Spectrosc.*, vol. 133, pp. 60–65, Dec. 2014.

[12] K. Bhuvaneswari *et al.*, "Enhanced photocatalytic activity of ethylenediamine-assisted tin oxide (SnO_2) nanorods for methylene blue dye degradation," *Mater. Lett.*, vol. 276, p. 128173, Oct. 2020.

[13] L.R. Hou, L. Lian, L. Zhou, L.H. Zhang, and C.Z. Yuan, "Interfacial hydrothermal synthesis of SnO_2 nanorods towards photocatalytic degradation of methyl orange," *Mater. Res. Bull.*, vol. 60, pp. 1–4, Dec. 2014.

[14] D. Narsimulu, E.S. Srinadhu, and N. Satyanarayana, "Surfactant-free microwave-hydrothermal synthesis of SnO_2 flower-like structures as an anode material for lithium-ion batteries," *Materialia*, vol. 4, pp. 276–281, Dec. 2018.

[15] S. Sharma and S. Chhoker, "CVD grown doped and Co-doped SnO_2 nanowires and its optical and electrical studies," *Mater. Today Proc.*, vol. 28, pp. 375–378, Jan. 2020.

[16] C. Gao, S. Yuan, B. Cao, and J. Yu, "SnO_2 nanotube arrays grown via an in situ template-etching strategy for effective and stable perovskite solar cells," *Chem. Eng. J.*, vol. 325, pp. 378–385, Oct. 2017.

[17] W. Matysiak, T. Tanski, and W. Smok, "Electrospinning as a versatile method of composite thin films fabrication for selected applications," *Solid State Phenom.*, vol. 293, pp. 35–49, 2019.

[18] T. Subbiah, G.S. Bhat, R.W. Tock, S. Parameswaran, and S.S. Ramkumar, "Electrospinning of nanofibers," *J. Appl. Polym. Sci.*, vol. 96, no. 2, pp. 557–569, Apr. 2005.

[19] T. Tański, W. Matysiak, and P. Jarka, "Introductory Chapter: Electrospinning-smart Nanofiber Mats," in *Electrospinning Method Used to Create Functional Nanocomposites Films*, InTech, 2018.

[20] W. Matysiak, T. Tański, and W. Smok, "Study of optical and dielectric constants of hybrid SnO_2 electrospun nanostructures," *Appl. Phys. A Mater. Sci. Process.*, vol. 126, no. 2, p. 115, Feb. 2020.

[21] Y. Zhang, X. He, J. Li, Z. Miao, and F. Huang, "Fabrication and ethanol-sensing properties of micro gas sensor based on electrospun SnO_2 nanofibers," *Sensors Actuators*, *B Chem.*, vol. 132, no. 1, pp. 67–73, May 2008.

[22] S.S. Mali *et al.*, "Synthesis of SnO_2 nanofibers and nanobelts electron transporting layer for efficient perovskite solar cells," *Nanoscale*, vol. 10, no. 17, pp. 8275–8284, May 2018.

[23] K. Zhang *et al.*, "An advanced electrocatalyst of Pt decorated SnO_2/C nanofibers for oxygen reduction reaction," *J. Electroanal. Chem.*, vol. 781, pp. 198–203, Nov. 2016.

[24] F. Li, T. Zhang, X. Gao, R. Wang, and B. Li, "Coaxial electrospinning heterojunction SnO_2/Au-doped In_2O_3 core-shell nanofibers for acetone gas sensor," *Sensors Actuators*, *B Chem.*, vol. 252, pp. 822–830, 2017.

[25] Z. Jiang *et al.*, "Highly sensitive acetone sensor based on Eu-doped SnO_2 electrospun nanofibers," *Ceram. Int.*, vol. 42, no. 14, pp. 15881–15888, Nov. 2016.

[26] J.Y. Cheong, C. Kim, J. W. Jung, K.R. Yoon, and I.D. Kim, "Porous SnO_2-CuO nanotubes for highly reversible lithium storage," *J. Power Sources*, vol. 373, pp. 11–19, Jan. 2018.

[27] Y.Y. Li, J.G. Wang, H.H. Sun, W. Hua, and X.R. Liu, "Heterostructured SnS_2/SnO_2 nanotubes with enhanced charge separation and excellent photocatalytic hydrogen production," *Int. J. Hydrogen Energy*, vol. 43, no. 31, pp. 14121–14129, Aug. 2018.

[28] Z. Huang, Z. Chen, S. Ding, C. Chen, and M. Zhang, "Enhanced conductivity and properties of SnO_2-graphene-carbon nanofibers for potassium-ion batteries by graphene modification," *Mater. Lett.*, vol. 219, pp. 19–22, May 2018.

[29] K. Wang and J. Huang, "Natural cellulose derived nanofibrous Ag-nanoparticle/SnO_2/carbon ternary composite as an anodic material for lithium-ion batteries," *J. Phys. Chem. Solids*, vol. 126, pp. 155–163, Mar. 2019.

[30] S. Javanmardi, S. Nasresfahani, and M.H. Sheikhi, "Facile synthesis of PdO/SnO_2/CuO nanocomposite with enhanced carbon monoxide gas sensing performance at low operating temperature," *Mater. Res. Bull.*, vol. 118, Oct. 2019.

[31] Y. Zhang, X. He, J. Li, Z. Miao, and F. Huang, "Fabrication and ethanol-sensing properties of micro gas sensor based on electrospun SnO_2 nanofibers," *Sensors Actuators*, *B Chem.*, vol. 132, no. 1, pp. 67–73, May 2008.

[32] W.Q. Li *et al.*, "Synthesis of hollow SnO_2 nanobelts and their application in acetone sensor," *Mater. Lett.*, vol. 132, pp. 338–341, Oct. 2014.

[33] L. Cheng *et al.*, "Synthesis and characterization of SnO_2 hollow nanofibers by electrospinning for ethanol sensing properties," *Mater. Lett.*, vol. 131, pp. 23–26, Sep. 2014.

[34] L. Liu *et al.*, "High toluene sensing properties of NiO-SnO_2 composite nanofiber sensors operating at 330°C," *Sensors Actuators*, *B Chem.*, vol. 160, no. 1, pp. 448–454, Dec. 2011.

[35] S.H. Yan *et al.*, "Synthesis of SnO_2-ZnO heterostructured nanofibers for enhanced ethanol gas-sensing performance," *Sensors Actuators*, *B Chem.*, vol. 221, pp. 88–95, Jul. 2015.

[36] F. Li, X. Gao, R. Wang, T. Zhang, and G. Lu, "Study on TiO_2-SnO_2 core-shell heterostructure nanofibers with different work function and its application in gas sensor," *Sensors Actuators*, *B Chem.*, vol. 248, pp. 812–819, 2017.

[37] S.W. Choi, J. Zhang, K. Akash, and S.S. Kim, "H_2S sensing performance of electrospun CuO-loaded SnO_2 nanofibers," *Sensors Actuators*, *B Chem.*, vol. 169, pp. 54–60, Jul. 2012.

[38] X. Xu *et al.*, "Effects of Al doping on SnO_2 nanofibers in hydrogen sensor," *Sensors Actuators*, *B Chem.*, vol. 160, no. 1, pp. 858–863, Dec. 2011.

[39] S.M. Hwang *et al.*, "A case study on fibrous porous SnO_2 anode for robust, high-capacity lithium-ion batteries," *Nano Energy*, vol. 10, pp. 53–62, Nov. 2014.

[40] W. Wang *et al.*, "Carbon-coated SnO_2@carbon nanofibers produced by electrospinning-electrospraying method for anode materials of lithium-ion batteries," *Mater. Chem. Phys.*, vol. 223, pp. 762–770, Feb. 2019.

[41] J. Zhu, G. Zhang, X. Yu, Q. Li, B. Lu, and Z. Xu, "Graphene double protection strategy to improve the SnO_2 electrode performance anodes for lithium-ion batteries," *Nano Energy*, vol. 3, pp. 80–87, Jan. 2014.

[42] Q. Wali, A. Fakharuddin, I. Ahmed, M.H. Ab Rahim, J. Ismail, and R. Jose, "Multiporous nanofibers of SnO2 by electrospinning for high efficiency dye-sensitized solar cells," *J. Mater. Chem. A*, vol. 2, no. 41, pp. 17427–17434, Nov. 2014.

[43] T. Tański, W. Matysiak, and Ł. Krzemiński, "Analysis of optical properties of TiO_2 nanoparticles and PAN/TiO_2 composite nanofibers," *Mater. Manuf. Process.*, vol. 32, no. 11, pp. 1218–1224, Aug. 2017.

[44] W. Matysiak, T. Tański, P. Jarka, M. Nowak, M. Kępińska, and P. Szperlich, "Comparison of optical properties of PAN/TiO_2, PAN/Bi_2O_3, and PAN/SbSI nanofibers," *Opt. Mater. (Amst).*, vol. 83, pp. 145–151, Sep. 2018.

[45] T. Tański, W. Matysiak, D. Kosmalska, and A. Lubos, "Influence of calcination temperature on optical and structural properties of TiO_2 thin films prepared by means of sol-gel and spin coating," *Bull. Pol. Acad. Sci. Tech. Sci.*, vol. 66, no. 2, pp. 151–156, Apr. 2018.

[46] W. Matysiak, T. Tański, and M. Zaborowska, "Manufacturing process and characterization of electrospun PVP/ZnO NPs nanofibers," *Bull. Pol. Acad. Sci. Tech. Sci.*, vol. 67, no. 2, pp. 193–200, 2019.

[47] W. Matysiak, T. Tański, and M. Zaborowska, "Manufacturing process, characterization and optical investigation of amorphous 1D zinc oxide nanostructures," *Appl. Surf. Sci.*, vol. 442, pp. 382–389, Jun. 2018.

[48] J. Muangban and P. Jaroenapibal, "Effects of precursor concentration on crystalline morphologies and particle sizes of electrospun WO_3 nanofibers," *Ceram. Int.*, vol. 40, no. 5, pp. 6759–6764, Jun. 2014.

[49] W. Matysiak and T. Tański, "Analysis of the morphology, structure and optical properties of 1D SiO_2 nanostructures obtained with sol-gel and electrospinning methods," *Appl. Surf. Sci.*, vol. 489, pp. 34–43, Sep. 2019.

[50] O.V. Otieno *et al.*, "Synthesis of TiO_2 nanofibers by electrospinning using water-soluble Ti-precursor," *J. Therm. Anal. Calorim.*, vol. 139, no. 1, pp. 57–66, Jan. 2020.

[51] N. Dharmaraj, C.H. Kim, K.W. Kim, H.Y. Kim, and E.K. Suh, "Spectral studies of SnO_2 nanofibres prepared by electrospinning method," *Spectrochim. Acta – Part A Mol. Biomol. Spectrosc.*, vol. 64, no. 1, pp. 136–140, May 2006.

[52] S.R. Ch, L. Zhang, T. Kang, Y. Lin, Y. Qiu, and S.R. A, "Annealing impact on the structural and optical properties of electrospun SnO_2 nanofibers for TCOs," *Ceram. Int.*, vol. 44, no. 5, pp. 4586–4591, Apr. 2018.

[53] S. Das, S. Kar, and S. Chaudhuri, "Optical properties of SnO_2 nanoparticles and nanorods synthesized by solvothermal process," *J. Appl. Phys.*, vol. 99, no. 11, p. 114303, Jun. 2006.

[54] N.S. Mohammad, "Understanding quantum confinement in nanowires: Basics, applications and possible laws," *J. Phys.-Condens. Matter*, vol. 26, no. 42. Institute of Physics Publishing, 22-Oct-2014.